RAA 2020 Vol. **20** No. **9**, 144(13pp) doi: 10.1088/1674–4527/20/9/144

http://www.raa-journal.org *http://iopscience.iop.org/raa*

Research in Astronomy and Astrophysics

Stability of the coplanar planetary four-body system

Chao Liu, Sheng-Ping Gong and Jun-Feng Li

School of Aerospace Engineering, Tsinghua University, Beijing 100084, China; *gongsp@tsinghua.edu.cn*

Received 2020 January 14; accepted 2020 April 6

Abstract We consider the coplanar planetary four-body problem, where three planets orbit a large star without the cross of their orbits. The system is stable if there is no exchange or cross of orbits. Starting from the Sundman inequality, the equation of the kinematical boundaries is derived. We discuss a reasonable situation, where two planets with known orbits are more massive than the third one. The boundaries of possible motions are controlled by the parameter c^2E. If the actual value of c^2E is less than or equal to a critical value $(c^2E)_{cr}$, then the regions of possible motions are bounded and therefore the system is stable. The criteria obtained in special cases are applied to the Solar System and the currently known extrasolar planetary systems. Our results are checked using N-body integrator.

Key words: methods: analytical — methods: numerical — celestial mechanics — planets and satellites: dynamical evolution and stability — stars: kinematics and dynamics — galaxies: kinematics and dynamics

1 INTRODUCTION

In our Solar System, eight planets orbit the Sun in the order of Mercury, Venus, Earth, Mars, Jupiter, Saturn, Uranus and Neptune. The moons also orbit their planets in the determined order. However, does this hierarchy of the Solar System stay unchanged? This problem has attracted much attention, and it has become a considerable challenge in celestial mechanics. Many concepts were introduced to solve this problem, such as Hill-type stability (Hill 1878), Lagrange stability (Sosnitskii 1999), Sundman stability (Lukyanov & Uralskaya 2012) and so on. In this paper, we will focus on Hill-type stability.

Previous studies of Hill-type stability have established several analytical criteria to judge the stability of the hierarchical system. The concept of Hill-type stability dates back to when Hill studied the Earth-Moon-Sun restricted three-body problem (Hill 1878). Hill wondered whether this Star-Planet-satellite system would remain in its hierarchy. To answer the question, Hill used the Jacobi integral of Moon to construct the boundaries of motions. As the zero-velocity surface around Earth is closed, Moon can never escape from Earth and become a planet of Sun, which means the system is Hill-type stable.

This concept has been extended to the general three-body problem (Golubev 1967, 1968a,b; Saari 1974, 1984, 1987; Marchal & Saari 1975; Bozis 1976; Zare 1976, 1977; Szebehely 1977; Szebehely & Zare 1977; Marchal & Bozis 1982; Sergysels 1986). In the general case, it is the parameter c^2E, where c is the angular momentum and E is the energy of the system, which controls the topology of the zero-velocity surface. The system is Hill-type stable if there is no exchange of bodies. There is a critical value of c^2E corresponding to the middle collinear equilibrium point. If the parameter c^2E of the system is less than or equal to the critical value, then the regions of possible motions are triply connected and there could be no exchange of bodies (i.e. the system is Hill-type stable).

The c^2E condition has been extensively applied to the hierarchical three-body system. Walker (1983b) investigated the stability of the star-planet-moon hierarchical three-body system. The hierarchical system, where $m_1 \gg m_2$, m_3 and m_1 form the inner binary with m_2, was sufficiently studied using two-body approximations for the angular momentum and the energy of the system (Donnison & Williams 1983, 1985; Donnison 1988, 2009, 2010, 2011). Petit et al. (2018) provided an inspiring method to understand the Hill-type stability in the framework of Angular Momentum Deficit. The Hill-type stability of a binary during encounters with a third star also was determined by using the c^2E condition (Donnison 1984b,a, 2006).

Four-body systems also widely exist in the Universe. Gong and Liu extended the concept of Hill-type stability to the four-body problem to study the stability of the hierarchical system (Gong & Liu 2016; Liu & Gong 2017b,a). In the (1-3) configuration four-body problem, where three bodies, constituting a subsystem, orbit a much larger body, the system is Hill-type stable if the three-body subsystem is Hill-type stable under the definition in the three-body problem (Gong & Liu 2016; Liu & Gong 2017a). In the (1-2-1) configuration four-body problem, where there is a binary subsystem, the system is Hill-type stable if there is no exchange of bodies between the binary and the third body (Liu & Gong 2017b). Under these definitions, if the criteria for Hill-type stability are satisfied, then the hierarchy of both four-body systems stay unchanged.

From this introduction, we know that the study of Hill-type stability provides an analytical method to judge whether the hierarchy of the system is stable in the three-body problem and the four-body problem. But the Hill-type stability criteria, derived in different models, are sufficient conditions but not necessary. In the four-body problem, only two kinds of configurations have been studied. In the $n(n \geq 5)$-body system, there is no definition of Hill-type stability. Thus, empirical stability criteria and numerical integration criteria have been proposed.

Walker et al., in a series of papers, outlined a method to study the empirical stability of the hierarchical n-body system (Walker et al. 1980; Walker & Roy 1981, 1983a; Walker 1983a; Walker & Roy 1983b). An expansion of the force function of the hierarchical n-body system was derived in terms of a set of $(n-1)(n-2)$ dimensionless parameters ϵ_{ki}, ϵ_{li}, which are representative of the size of the disturbances on the Keplerian orbits of various bodies. The parameter Σ_i, in terms of ϵ_{ki} and ϵ_{li}, interpreted to be a measure of the disturbance placed on the orbit of m_i by other masses in the system. Generally, if each Σ_i is less than 10^{-2}, the hierarchical system is empirical stable.

The numerical work involves a wide range of simulations of the system. Most of the works focused on the three-body system and devoted to determining the boundary of stability (Harrington 1972; Donnison & Mikulskis 1992, 1994). In the $n(n \geq 4)$-body problem, the multi-planet systems are always unstable with respect to close encounters if the initial semi-major axis difference, Δ, is less than 10 (Chambers et al. 1996). The time of first close encounter is given approximately by $\log t = b\Delta + c$, where b and c are constants. Subsequently, many researchers (Duncan & Lissauer 1997; Faber & Quillen 2007; Smith & Lissauer 2009; Obertas et al. 2017) further discussed the approximate stability time for a system which was taken to be the time when the orbits of two or more planets crossed. Tamayo et al. (2016) also provided a method to predict the stability of tightly packed planetary systems using optimized machine-learning classifiers.

In this work, we study the stability of the planetary four-body system, where three planets orbit a large star. The mass of the star is much greater than the planets, and the orbits of the planets do not cross at initial. The stability of the system is defined as:

If there is no exchange or cross of orbits of the planets, the planetary four-body system is stable.

Based on the definition, two analytical stability criteria are derived in different situations, and then applied to the Solar System and extrasolar systems.

2 THE COPLANAR PLANETARY FOUR BODY MODEL

The four body system includes a massive star with three much smaller planets orbiting in a planetary hierarchy, which is shown in Figure 1. Here, P_i denotes the position of the i-th body, while m_i denotes the mass. The Jacobian coordinates, ρ_i, $i = 1, 2, 3$, are defined as

$$\rho_1 = \left|\overrightarrow{P_0P_1}\right|, \rho_2 = \left|\overrightarrow{P_{01}P_2}\right|, \rho_3 = \left|\overrightarrow{P_{012}P_3}\right|, \tag{1}$$

where P_{01} is the barycenter of P_0 and P_1, and P_{012} is the barycenter of P_{01} and P_2.

The motions of the system are determined by the famous Sundman inequality (Sundman 1912), which is given by

$$2E - 2U - \frac{c^2}{K} \geq 0, \tag{2}$$

where E is the total energy of the system, U is the potential energy, c is the angular momentum and K denotes the moment of inertia. The expression of the potential energy is

$$U = -G\left(\frac{m_0m_1}{r_{01}} + \frac{m_0m_2}{r_{02}} + \frac{m_1m_2}{r_{12}} + \frac{m_0m_3}{r_{03}} + \frac{m_1m_3}{r_{13}} + \frac{m_2m_3}{r_{23}}\right), \tag{3}$$

where G is the gravitational constant and

$$r_{ij} = \left|\overrightarrow{P_iP_j}\right|, \quad i < j. \tag{4}$$

The moment of inertia can be given by (Gong & Liu 2016)

$$K = \frac{m_0m_1}{M_1}\rho_1^2 + \frac{M_1m_2}{M_2}\rho_2^2 + \frac{M_2m_3}{M_3}\rho_3^2, \tag{5}$$

where $M_i = \Sigma_{k=0}^{i} m_k$, $i = 0, 1, 2, 3$.

The stability of the system is ensured if there is no cross of the orbits or exchange of the order of the planets. In other words, it requires that the regions of possible motions of P_1 are contained by the orbit of P_2 and meanwhile the motions of P_3 are restricted outside. Considering the reference frame rotating with P_0 and P_2. Their barycenter, P_{02}, is fixed at the origin of the coordinate system; the x axis points from P_0 to P_2; and the y axis forms a right triad with the x axis.

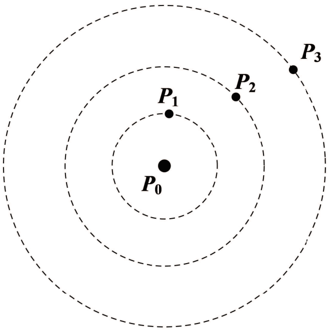

Fig. 1 The coplanar planetary four body system.

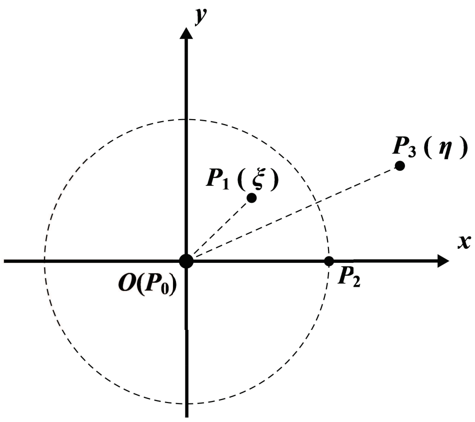

Fig. 2 The four body system in the complex plane.

As

$$m_0 \gg m_i, i = 1, 2, 3, \tag{6}$$

it is reasonable to assume that

$$r_{01} \approx \rho_1, \quad r_{02} \approx \rho_2, \quad r_{03} \approx \rho_3. \tag{7}$$

Denote the coordinates of P_1 and P_3 as (x_1, y_1), (x_3, y_3), respectively. Then, we introduce two complex variables as

$$\boldsymbol{\xi} = \frac{x_1}{\rho_2} + i\frac{y_1}{\rho_2}, \tag{8}$$

$$\boldsymbol{\eta} = \frac{x_3}{\rho_2} + i\frac{y_3}{\rho_2}. \tag{9}$$

Based on the geometrical relationship, we obtain

$$\begin{cases} r_{02} = \rho_2, & r_{01} = |\boldsymbol{\xi}|\,\rho_2, \\ r_{03} = |\boldsymbol{\eta}|\,\rho_2, & r_{12} = |\boldsymbol{\xi} - 1|\,\rho_2, \\ r_{23} = |\boldsymbol{\eta} - 1|\,\rho_2, & r_{13} = |\boldsymbol{\xi} - \boldsymbol{\eta}|\,\rho_2. \end{cases} \tag{10}$$

Substitute Equations (3), (5), (7), and (10) into Equation (2), and it becomes

$$2E\rho_2^2 + 2GP(\boldsymbol{\xi}, \boldsymbol{\eta})\,\rho_2 - \frac{c^2}{Q(\boldsymbol{\xi}, \boldsymbol{\eta})} \geq 0, \tag{11}$$

where

$$\begin{aligned} P(\boldsymbol{\xi}, \boldsymbol{\eta}) = &\frac{m_0 m_1}{|\boldsymbol{\xi}|} + m_0 m_2 + \frac{m_1 m_2}{|\boldsymbol{\xi} - 1|} + \frac{m_0 m_3}{|\boldsymbol{\eta}|} \\ &+ \frac{m_1 m_3}{|\boldsymbol{\xi} - \boldsymbol{\eta}|} + \frac{m_2 m_3}{|\boldsymbol{\eta} - 1|}, \end{aligned} \tag{12}$$

$$Q(\boldsymbol{\xi}, \boldsymbol{\eta}) = \frac{m_0 m_1}{M_1}|\boldsymbol{\xi}|^2 + \frac{M_1 m_2}{M_2} + \frac{M_2 m_3}{M_3}|\boldsymbol{\eta}|^2. \tag{13}$$

Inequality (11) represents the regions of possible motions whose boundaries are determined by a quadratic equation in ρ_2. If $E \geq 0$, then there must be a body in the system not moving on a closed orbit. This situation is not considered in this work. So we only consider the case that $E < 0$. As $\rho_2 > 0$, the discriminant of roots must be non-negative, which means

$$\Delta = 4G^2P^2(\boldsymbol{\xi}, \boldsymbol{\eta}) + \frac{8c^2E}{Q(\boldsymbol{\xi}, \boldsymbol{\eta})} \geq 0. \tag{14}$$

Inequality (14) gives the constraint of possible motions of P_1 and P_3, in terms of the coordinates $\boldsymbol{\xi}$ and $\boldsymbol{\eta}$ in the complex plane. The schematic of the system in the complex plane is shown in Figure 2. If the conditions,

$$|\boldsymbol{\xi}| < 1, \quad |\boldsymbol{\eta}| > 1, \tag{15}$$

always hold, the hierarchy of the system will never change which makes the stability ensured.

The condition for equality of inequality (14) can be rewritten as

$$c^2E = -\frac{G^2P^2(\boldsymbol{\xi}, \boldsymbol{\eta})\,Q(\boldsymbol{\xi}, \boldsymbol{\eta})}{2}, \tag{16}$$

which means the boundaries of the regions of possible motions are controlled by the parameter c^2E. In the three body problem the parameter c^2E determines the topology of the regions of possible motions of the third body, but here it limits the motions of both P_1 and P_3.

Note that there are four dimensions because the coordinates $\boldsymbol{\xi}$ and $\boldsymbol{\eta}$ are unknown, which makes it difficult to draw the boundaries. Therefore, we consider two special cases that the orbits of P_2 and P_3 (or P_2 and P_1) are determined.

3 STABILITY CRITERIA WITH ORBITS OF TWO PLANETS DETERMINED

In some planetary four-body system, it happens that two of the planets are more massive than the third one and their orbits are considered unchanged for a long time. In this case, it is not necessary to study the stability of the massive planets in the four-body model, because the smaller planet has little influence on the motions of the massive planets. We only need to study the motions of the third smaller planet when we investigate the stability of the system. Back to our model, if the orbits of the two massive planets, P_2 and P_3 (or P_2 and P_1), are determined, the values of variable $\boldsymbol{\eta}$ (or $\boldsymbol{\xi}$) are also determined. Then, the regions of possible motions of another planet can be obtained by Equation (16).

3.1 Determining the Orbits of P_2 and P_3

If the orbits of P_2 and P_3 are known and unchanged, and there is no exchange of the orbits of P_2 and P_3, then $\boldsymbol{\eta}$ is no longer a variable but a parameter in Equation (16), and $|\boldsymbol{\eta}| > 1$. Equation (16) determines the zero velocity curves and hence regions of possible motions of P_1 in the complex plane. For a certain value of parameters $\boldsymbol{\eta}$, the motions of P_1 in the complex plane are determined by the parameter c^2E, which is shown in Figure 3.

In Figure 3(a), the inner zero velocity curve is closed and it does not contain the second planet P_2. The motions of P_1 are bounded and it can never exchange the orbits with P_2 or be captured by P_2, which means that the system is stable under the definition. The smaller values of c^2E make the inner zero velocity curve smaller and hence the stability of the system better. In Figure 3(b), the inner zero velocity curve contains the second planet P_2. P_1 can exchange the orbits with P_2 or be captured by P_2, and in this case the stability is uncertain. The increases of values of c^2E will extend the inner zero velocity curve and finally, the regions of possible motions will be simply connected.

Figure 3(c) shows the critical case that the two regions of possible motions around P_0 and P_2 turn from disconnected to connected. Figure 3(d) is the local curve around P_2 in the critical case. The bifurcation of the curves happens at the equilibrium point to the left side of P_2. The equilibrium points are given by Zare (1977)

$$\begin{cases} \Delta(\boldsymbol{\xi};\boldsymbol{\eta}) = 0, \\ \dfrac{d}{d\boldsymbol{\xi}}\Delta(\boldsymbol{\xi};\boldsymbol{\eta}) = 0. \end{cases} \tag{17}$$

Substitution of Equation (14) into Equation (17) gives

$$\begin{cases} c^2E = -\dfrac{G^2P^2(\boldsymbol{\xi};\boldsymbol{\eta})\,Q(\boldsymbol{\xi};\boldsymbol{\eta})}{2}, \\ Q\left[\dfrac{m_0m_1\boldsymbol{\xi}}{|\boldsymbol{\xi}|^3} + \dfrac{m_1m_2(\boldsymbol{\xi}-1)}{|\boldsymbol{\xi}-1|^3} + \dfrac{m_1m_3(\boldsymbol{\xi}-\boldsymbol{\eta})}{|\boldsymbol{\xi}-\boldsymbol{\eta}|^3}\right] \\ \quad -\dfrac{Pm_0m_1}{M_1}\boldsymbol{\xi} = 0. \end{cases} \tag{18}$$

From the second of Equation (18), we can obtain the coordinates $\boldsymbol{\xi}_e$ of the equilibrium point to the left side of P_2 numerically. Note that the solutions of $\boldsymbol{\xi}_e$ are associated with the values of parameter $\boldsymbol{\eta}$ which is shown in Figure 4a. The absolute value of imaginary part of $\boldsymbol{\xi}_e$ is much less than 1, so that in Figure 4(b) we use $|\boldsymbol{\xi}_e|$ as the z-axis.

The first line of Equation (18) gives the expression of the critical values of c^2E. The critical values, denoted as $(c^2E)_{cr,\boldsymbol{\eta}}$, is associated with the equilibrium point $\boldsymbol{\xi}_e$ and hence the values of parameter $\boldsymbol{\eta}$. The relations between $(c^2E)_{cr,\boldsymbol{\eta}}$ with $\boldsymbol{\eta}$ are shown in Figure 4(c). The positions of P_3 have an influence on the value of $(c^2E)_{cr,\boldsymbol{\eta}}$, and the minimum of $(c^2E)_{cr,\boldsymbol{\eta}}$ is denoted as

$$(c^2E)_{cr} = \min_{\boldsymbol{\eta}\in\Omega}\left((c^2E)_{cr,\boldsymbol{\eta}}\right), \tag{19}$$

where Ω is the range of $\boldsymbol{\eta}$. For example, in Figure 4 $\Omega = \{\boldsymbol{\eta} : \boldsymbol{\eta} \in \mathbb{C}, 1.6 \le |\boldsymbol{\eta}| \le 2.4\}$, where $\mathbb{C}$ is the complex field.

If the value of c^2E of the system is less than or equal to $(c^2E)_{cr}$, the motions of P_1 are limited inside of the orbits of P_2, which is similar to the case shown in Figure 3(a). Besides, there is no exchange of the orbits of P_2 and P_3 based on the assumptions. Thus, the stability of the system is ensured. The stability criterion can be summarized as follows.

Criterion I:

In the coplanar planetary four-body problem, three planets, P_1, P_2, P_3, orbit the star in a planetary hierarchy. P_2, P_3 are more massive than P_1 and the orbits of two massive planets are determined. The system is stable if

$$(c^2E)_{ac} \le (c^2E)_{cr}, \tag{20}$$

where $(c^2E)_{ac}$ is the actual value of c^2E of the system and $(c^2E)_{cr}$ is given by Equation (19).

Based on the condition (6), it is possible to express the real component of $\boldsymbol{\xi}_e$ and hence $(c^2E)_{cr}$ in a closed form. Denote $\boldsymbol{\xi}_e = x_e + iy_e$. As shown in Figure 4(a), y_e is very small compared to x_e and has little effect on the value of $(c^2E)_{cr}$. Thus, we can set $\boldsymbol{\xi} = x$, where x is real and $0 < x < 1$, and then the solution of the second of Equation (18), denoted as $\boldsymbol{\xi}_a$, is an approximation of $\boldsymbol{\xi}_e$.

The equilibrium point lies to the left side of P_2. Denote

$$x = 1 - \mu, \tag{21}$$

where $\mu > 0$ and usually $\mu < 0.1$. Substituting $\boldsymbol{\xi} = 1 - \mu$ and after some simplifications, the second of Equation (18) becomes

$$\left[m_1(1-\mu)^2 + m_2 + m_3|\boldsymbol{\eta}|^2\right]\left[\frac{m_0m_1}{(1-\mu)^2} - \frac{m_1m_2}{\mu^2}\right] - m_1(1-\mu)\left[\frac{m_0m_1}{1-\mu} + m_0m_2 + \frac{m_1m_2}{\mu} + \frac{m_0m_3}{|\boldsymbol{\eta}|}\right] = 0. \tag{22}$$

Then, by multiplying both sides of Equation (22) by $(1-\mu)^2\mu^2$, it becomes a univariate equation of five degrees, which is

$$\Sigma_{i=0}^{5} c_i\mu^i = 0, \tag{23}$$

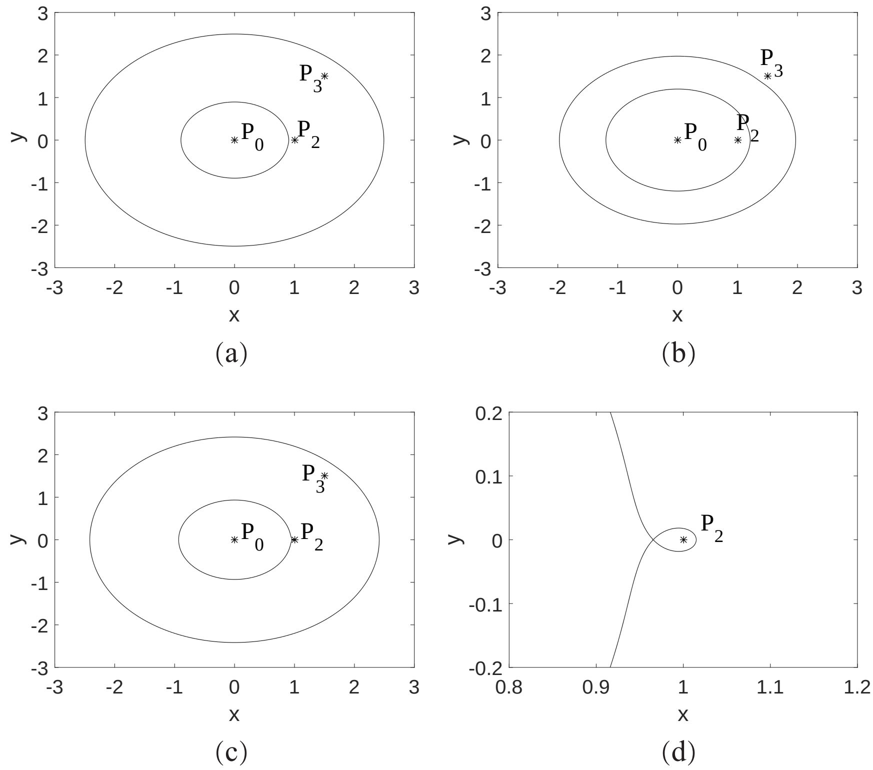

Fig. 3 Zero velocity curves of P_2 for different values of c^2E. (a) $c^2E = -6.10 \times 10^{-9}$, (b) $c^2E = -5.95 \times 10^{-9}$, (c) $c^2E = -6.0724345 \times 10^{-9}$, (d) $c^2E = -6.0724345 \times 10^{-9}$, around P_3. $G = 1$, $m_0 = 1$, $m_1 = 9.55206 \times 10^{-5}$, $m_2 = m_3 = 9.55206 \times 10^{-4}$, $\boldsymbol{\eta} = 1.5 + 1.5i$.

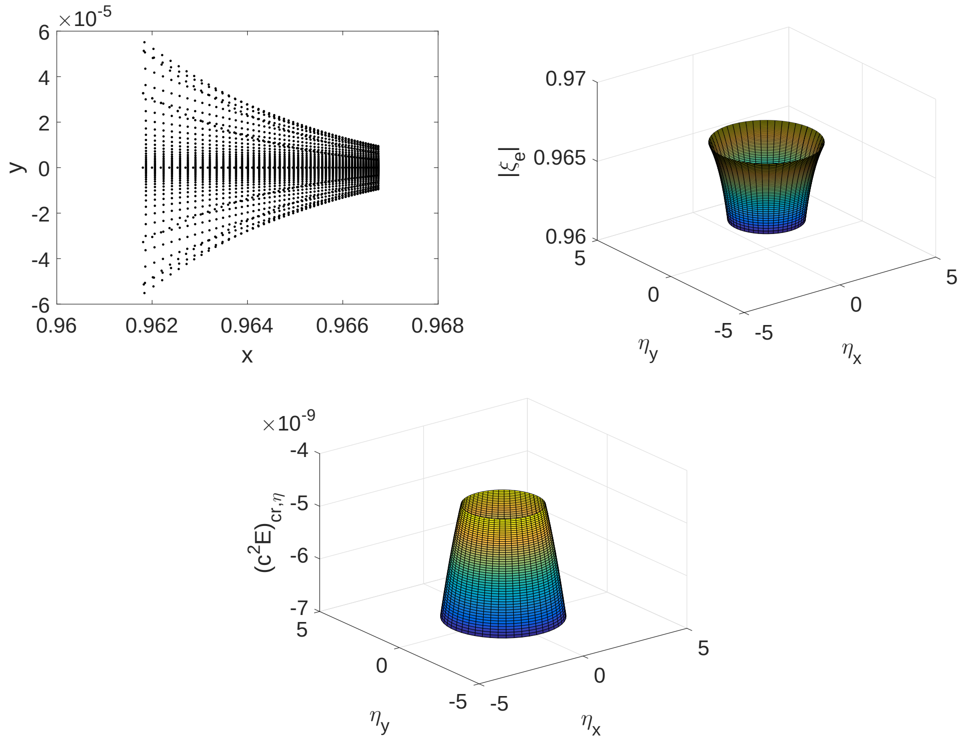

Fig. 4 The relations between $\boldsymbol{\xi}_e$, $(c^2E)_{cr,\boldsymbol{\eta}}$ with $\boldsymbol{\eta}$. (a) The solutions of $\boldsymbol{\xi}_e$ on the complex plane, (b) $\eta_x - \eta_y - |\boldsymbol{\xi}_e|$ surface, (c) $\eta_x - \eta_y - (c^2E)_{cr,\boldsymbol{\eta}}$ surface. $G = 1$, $m_0 = 1$, $m_1 = 9.55206 \times 10^{-5}$, $m_2 = m_3 = 9.55206 \times 10^{-4}$, $1.6 \leq |\boldsymbol{\eta}| \leq 2.4$. η_x denotes the real component of $\boldsymbol{\eta}$ while η_y denotes the imaginary component.

where

$$\begin{cases} c_5 = \epsilon_2 + \epsilon_3/\left|\boldsymbol{\eta}\right|, \\ c_4 = -3\epsilon_2 - 3\epsilon_3/\left|\boldsymbol{\eta}\right|, \\ c_3 = 3\epsilon_2 + 3\epsilon_3/\left|\boldsymbol{\eta}\right|, \\ c_2 = (\left|\boldsymbol{\eta}\right|^2 - 1/\left|\boldsymbol{\eta}\right|)\epsilon_3, \\ c_1 = 3\epsilon_1\epsilon_2 + 2\epsilon_2^2 + 2\left|\boldsymbol{\eta}\right|^2\epsilon_2\epsilon_3, \\ c_0 = -\epsilon_1\epsilon_2 - \epsilon_2^2 - \left|\boldsymbol{\eta}\right|^2\epsilon_2\epsilon_3, \end{cases} \tag{24}$$

and

$$\epsilon_1 = \frac{m_1}{m_0}, \quad \epsilon_2 = \frac{m_2}{m_0}, \quad \epsilon_3 = \frac{m_3}{m_0}. \tag{25}$$

In Equation (24) only the main items in the coefficients c_i are retained while the items with relatively smaller values are omitted. Furthermore, as m_0 is much larger than other bodies, the magnitude of the coefficients can be divided into different levels. The coefficients with a relatively large order of magnitude are c_5, c_4, c_3, while c_0 is in the order of ϵ_i^2. The order of c_1 and c_2 is associated with the parameter $|\boldsymbol{\eta}|$.

The Hill sphere around P_2 is much smaller compared to the sphere around P_0 as $m_0 \gg m_2$, which means $\mu \ll 1$. We keep the smallest power in μ with the associated coefficient for the group of c_5, c_4, c_3. Therefore, the terms with the associated coefficient c_5 and c_4 are neglected. Thus Equation (23) can be reduced to

$$c_3\mu^3 + c_2\mu^2 + c_1\mu + c_0 = 0. \tag{26}$$

The first and second order terms are retained as their coefficients c_1 and c_2 are related to the value of $|\boldsymbol{\eta}|$. This makes the relative error much bigger if they are ignored.

Equation (26) is a cubic polynomial of μ and its roots can be solved using Cardano's Formula. Therefore, an approximation to the solution of Equation (22) is given by

$$\mu_a = \left(-\frac{q}{2} + \sqrt{\Delta}\right)^{1/3} + \left(-\frac{q}{2} - \sqrt{\Delta}\right)^{1/3} - \frac{c_2}{3c_3}, \tag{27}$$

where

$$\begin{cases} p = \dfrac{3c_3c_1 - c_2^2}{3c_3^2}, \\ q = \dfrac{27c_3^2c_0 - 9c_3c_2c_1 + 2c_2^3}{27c_3^3}, \end{cases} \tag{28}$$

and the discriminant of the cubic equation is

$$\Delta = (p/3)^3 + (q/2)^2. \tag{29}$$

Then, the first line of Equation (18) can be expanded at the approximate solution $\boldsymbol{\xi}_a = 1 - \mu_a$, which is

$$\begin{aligned} \left(c^2E\right)_{cr,\boldsymbol{\eta}} = \left(c^2E\right)_{\boldsymbol{\xi}_a} + \left(c^2E\right)'_{\boldsymbol{\xi}_a}(\boldsymbol{\xi}_e - \boldsymbol{\xi}_a) \\ + O\left((\boldsymbol{\xi}_e - \boldsymbol{\xi}_a)^2\right), \end{aligned} \tag{30}$$

where $\boldsymbol{\xi}_e$ denotes the exact solution of the second of Equation (18). Meanwhile, $\boldsymbol{\xi}_a = 1 - \mu_a$ is the approximation of the bifurcation point of the zero velocity surface, so $\left(c^2E\right)'_{\boldsymbol{\xi}_a} \approx 0$. Then Equation (30) becomes

$$\left(c^2E\right)_{cr,\boldsymbol{\eta}} = \left(c^2E\right)_{\boldsymbol{\xi}_a} + O\left((\boldsymbol{\xi}_e - \boldsymbol{\xi}_a)^2\right). \tag{31}$$

Thus, Equation (19) can be rewritten as

$$\begin{aligned} \left(c^2E\right)_{cr} = -\frac{G^2m_0^5}{2} \\ \max_{\boldsymbol{\eta}\in\Omega}\left\{ \begin{aligned} \left(\frac{\epsilon_1}{1-\mu_a} + \epsilon_2 + \frac{\epsilon_1\epsilon_2}{\mu_a} + \frac{\epsilon_3}{|\boldsymbol{\eta}|}\right)^2 \times \\ \times\left[\epsilon_1(1-\mu_a)^2 + \epsilon_2 + \epsilon_3|\boldsymbol{\eta}|^2\right] \end{aligned} \right\}, \end{aligned} \tag{32}$$

where Ω is the range of $\boldsymbol{\eta}$.

The value of $(c^2E)_{cr}$ monotone decreases with $|\boldsymbol{\eta}|$ if

$$|\boldsymbol{\eta}| \geq \left(\frac{\epsilon_1(1-\mu_a)^2 + \epsilon_2}{\epsilon_1/(1-\mu_a) + \epsilon_2 + \epsilon_1\epsilon_2/\mu_a}\right)^{1/3}. \tag{33}$$

The right side of inequality (33) is less than 1, as P_3 is located outside of the orbit of P_2, i.e., $|\boldsymbol{\eta}| > 1$. Therefore, denote $r_m = \max|\boldsymbol{\eta}|$, and Equation (32) becomes

$$\begin{aligned} \left(c^2E\right)_{cr} = -\frac{G^2m_0^5}{2} \\ \left\{ \begin{aligned} \left(\frac{\epsilon_1}{1-\mu_a} + \epsilon_2 + \frac{\epsilon_1\epsilon_2}{\mu_a} + \frac{\epsilon_3}{r_m}\right)^2 \times \\ \times\left[\epsilon_1(1-\mu_a)^2 + \epsilon_2 + \epsilon_3 r_m^2\right] \end{aligned} \right\}. \end{aligned} \tag{34}$$

The value determined by Equation (34) also is an approximation of the exact critical value. The accuracy has been verified with the results shown in Figure 5. The relative error compared to the exact value tends to be less than 10^{-5} which means the approximation is also reasonable.

In Criterion I, the actual value $(c^2E)_{ac}$ is based on the total energy E and the corresponding angular momentum c of the system. Using two body approximation, the energy is (Liu & Gong 2017a):

$$E = -\frac{G}{2}\left(\frac{m_0m_1}{a_1} + \frac{M_1m_2}{a_2} + \frac{M_2m_3}{a_3}\right), \tag{35}$$

and the corresponding angular momentum is

$$\begin{aligned} c = G^{1/2}\{m_0m_1(a_1(1-e_1^2)/M_1)^{1/2} \\ + M_1m_2(a_2(1-e_2^2)/M_2)^{1/2} \\ + M_2m_3(a_3(1-e_3^2)/M_3)^{1/2}\}, \end{aligned} \tag{36}$$

where a_i and e_i ($i = 1, 2, 3$) are the semi-major axis and eccentricity of P_i, respectively.

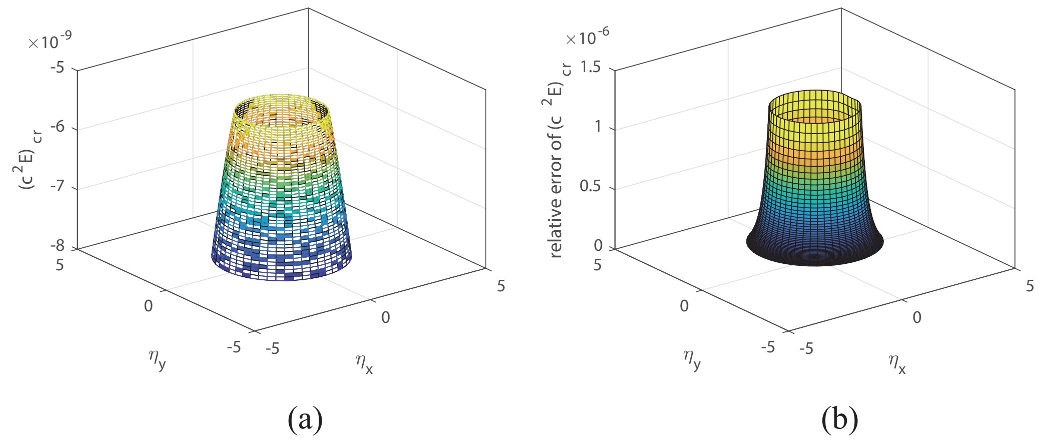

Fig. 5 Comparison of the approximation and the exact solution of $(c^2E)_{cr}$. (a) Approximation and exact solution of $(c^2E)_{cr}$, (b) relative error of $(c^2E)_{cr}$. $G = 1$, $m_0 = 1$, $m_1 = 10^{-4}$, $m_2 = 10^{-3}$, $m_3 = 10^{-3}$, and $1.6 < |\boldsymbol{\eta}| < 2.4$. In Fig. 5(a) the two surfaces are too close to distinguish. Fig. 5(b) shows the relative error between the approximation and the exact value of $(c^2E)_{cr}$.

Thus, we have

$$(c^2E)_{ac} = -\frac{G^2m_0^5}{2}(\epsilon_1/\alpha_{12} + \epsilon_2 + \epsilon_3/\alpha_{32}) \times \left[\epsilon_1\sqrt{\alpha_{12}(1-e_1^2)} + \epsilon_2\sqrt{1-e_2^2} + \epsilon_3\sqrt{\alpha_{32}(1-e_3^2)}\right]^2, \tag{37}$$

where

$$\alpha_{ij} = \frac{a_i}{a_j}, \quad i,j = 1,2,3. \tag{38}$$

Then the stability condition (20) given in Criterion I can be rewritten as

$$A(1-e_1^2) + B\sqrt{1-e_1^2} + C \geq 0, \tag{39}$$

where

$$\begin{cases} A = (\epsilon_1/\alpha_{12} + \epsilon_2 + \epsilon_3/\alpha_{32})\,\epsilon_1^2\alpha_{12}, \\ B = 2\left[\epsilon_2\sqrt{1-e_2^2} + \epsilon_3\sqrt{\alpha_{32}(1-e_3^2)}\right] \\ \quad \times (\epsilon_1/\alpha_{12} + \epsilon_2 + \epsilon_3/\alpha_{32})\,\epsilon_1\sqrt{\alpha_{12}}, \\ C = \left[\epsilon_2\sqrt{1-e_2^2} + \epsilon_3\sqrt{\alpha_{32}(1-e_3^2)}\right]^2 \\ \quad \times (\epsilon_1/\alpha_{12} + \epsilon_2 + \epsilon_3/\alpha_{32}) \\ \quad - \left(\frac{\epsilon_1}{1-\mu_a} + \epsilon_2 + \frac{\epsilon_1\epsilon_2}{\mu_a} + \frac{\epsilon_3}{r_m}\right)^2 \\ \quad \times \left[\epsilon_1(1-\mu_a)^2 + \epsilon_2 + \epsilon_3 r_m^2\right]. \end{cases} \tag{40}$$

If $C \geq 0$ inequality (39) holds as $A > 0$ and $B > 0$. If $C < 0$, this gives a solution of the form

$$e_1 \leq \sqrt{1 - \left(\frac{-B + \sqrt{B^2 - 4AC}}{2A}\right)^2}. \tag{41}$$

The $\alpha_{12} - e_1$ curves for different value of α_{32} is shown in Figure 6. The regions on the left side of the curves are stable. The inner planet with a small eccentricity is more likely to be stable. The stable regions become larger if the parameter α_{32} decreases. The relations between α_{32} and α_{12} are shown in Figure 7. The region on the left side of the curve is ensured to be stable with the conditions $\alpha_{32} > 1$ and $\alpha_{12} < 1$. The plot makes it clear that with the increases of the parameter α_{32} the value of α_{12} decreases which means the ensured stable regions have shrunk. Besides, $r_m = \alpha_{32}(1 + e_3)/(1 - e_2)$ under the definition.

It needs to be pointed out that Sundman inequality is a necessary condition for the possible motions so that the stability criterion is sufficient but not necessary. We can conclude that the stable regions in Figure 6 absolutely are stable. Nevertheless, the real stable regions may be larger than that the criterion gives. Therefore, the trend shown in Figure 7 represents the results of the criterion but it may be not real situations.

If $m_3 = 0$, the problem degenerates into a three-body case. Similarly, the stable regions in the $\alpha_{12} - e_1$ plane are shown in Figure 8. The solid line is the boundary of the three-body problem while the others are the boundaries for different α_{32} in the four-body case. In general, the third planet reduces the stable regions of the inner planet which makes the stability worse.

3.2 Determining the Orbits of P_1 and P_2

If P_1 and P_2 are massive and their orbits are determined without exchange of orbits , $\boldsymbol{\xi}$ is no longer a variable but a parameter in Equation (16), and $|\boldsymbol{\xi}| < 1$. Equation (16) determines the zero velocity curves and hence regions of

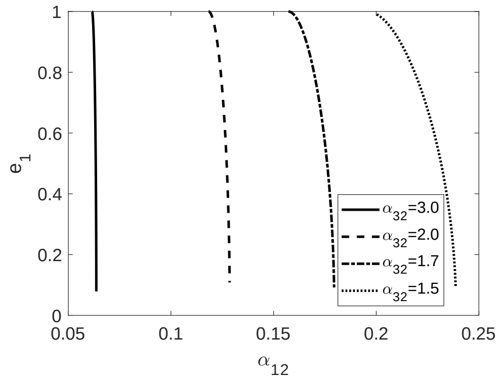

Fig. 6 The $\alpha_{12} - e_1$ curves for different values of α_{32}. The parameters of the system are given as $G = 1$, $m_0 = 1$, $m_1 = 10^{-4}$, $m_2 = 10^{-3}$, $m_3 = 10^{-3}$, $e_2 = 0.02$, and $e_3 = 0.02$. Here $\alpha_{12} = a_1/a_2$ and $\alpha_{32} = a_3/a_2$. The regions on the left side of the curves are ensured to be stable.

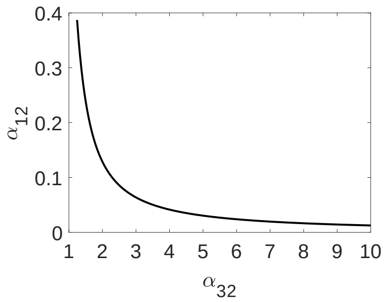

Fig. 7 The $\alpha_{32} - \alpha_{12}$ curve. The parameters of the system are given as $G = 1$, $m_0 = 1$, $m_1 = 10^{-4}$, $m_2 = 10^{-3}$, $m_3 = 10^{-3}$, and $e_1 = e_2 = e_3 = 0.02$. Here $\alpha_{12} = a_1/a_2$ and $\alpha_{32} = a_3/a_2$. The regions on the left side of the curve are ensured to be stable with the conditions $\alpha_{32} > 1$ and $\alpha_{12} < 1$.

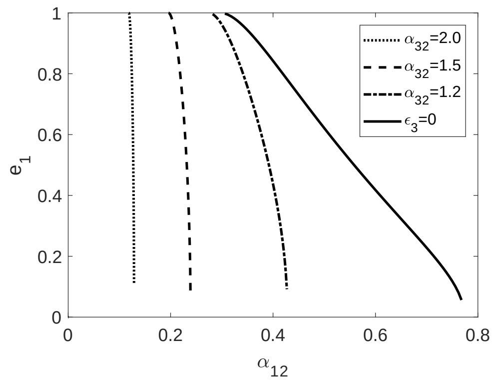

Fig. 8 The $\alpha_{12} - e_1$ curves. The parameters of the four-body system are given as $G = 1$, $m_0 = 1$, $m_1 = 10^{-4}$, $m_2 = 10^{-3}$, $m_3 = 10^{-3}$, and $e_1 = e_2 = 0.02$. Here $\alpha_{12} = a_1/a_2$ and $\alpha_{32} = a_3/a_2$. For the three-body case, $m_3 = 0$. The regions on the left side of the curves are ensured to be stable.

possible motions of P_3 in the complex plane. For a certain value of parameters $\boldsymbol{\xi}$, the motions of P_3 in the complex plane are determined by the parameter c^2E, which is shown in Figure 9.

In Figure 9(a), the outer zero velocity curve is closed and contains the second planet P_2. P_3 is located at the outside and can never exchange the orbits with P_2 or be captured by P_2, which means the system is stable under the definition. The smaller values of c^2E will extend the outer zero velocity curve and make the stability of the system better. In Figure 9(b), the outer region of possible motions contains the second planet P_2. P_3 can exchange the orbits with P_2 or be captured by P_2, and the stability is not ensured in this case. The increases of values of c^2E will extend both the inner region and outer region of possible motions of P_3. Finally, the regions of possible motions will be simply connected.

Figure 9(c) shows the critical case that the outer region and the region around P_2 turn from disconnected to connected. Figure 9(d) is the local curve around P_2 in the critical case. The bifurcation of the curves happens at the equilibrium point to the right side of P_2. The equilibrium points are given by Zare (1977)

$$\begin{cases} \Delta(\boldsymbol{\eta};\boldsymbol{\xi}) = 0, \\ \dfrac{d}{d\boldsymbol{\eta}}\Delta(\boldsymbol{\eta};\boldsymbol{\xi}) = 0. \end{cases} \tag{42}$$

Substituting Equation (14) into Equation (42) gives

$$\begin{cases} c^2E = -\dfrac{G^2P^2(\boldsymbol{\eta};\boldsymbol{\xi})\,Q(\boldsymbol{\eta};\boldsymbol{\xi})}{2}, \\ Q\left[\dfrac{m_0m_3\boldsymbol{\eta}}{|\boldsymbol{\eta}|^3} + \dfrac{m_1m_3(\boldsymbol{\eta}-\boldsymbol{\xi})}{|\boldsymbol{\eta}-\boldsymbol{\xi}|^3} + \dfrac{m_2m_3(\boldsymbol{\eta}-1)}{|\boldsymbol{\eta}-1|^3}\right] \\ \quad -\dfrac{PM_2m_3}{M_3}\boldsymbol{\eta} = 0. \end{cases} \tag{43}$$

From the second of Equation (43), we can obtain the coordinates $\boldsymbol{\eta}_e$ of the equilibrium point to the right side of P_2 numerically. Similarly to the work in Section 3.1, the solutions of $\boldsymbol{\eta}_e$ are associated with the values of parameter $\boldsymbol{\xi}$. The absolute value of imaginary part of $\boldsymbol{\eta}_e$ is much less than 1.

The critical values, denoted as $(c^2E)_{cr,\boldsymbol{\xi}}$, is associated with the equilibrium point $\boldsymbol{\eta}_e$ and hence the values of parameter $\boldsymbol{\xi}$. The positions of P_1 have an influence on the value of $(c^2E)_{cr,\boldsymbol{\xi}}$, and the minimum of $(c^2E)_{cr,\boldsymbol{\xi}}$ is denoted as

$$(c^2E)^*_{cr} = \min_{\boldsymbol{\xi}\in\Omega^*}\left((c^2E)_{cr,\boldsymbol{\xi}}\right), \tag{44}$$

where Ω^* is the value range of $\boldsymbol{\xi}$.

If the value of c^2E of the system is less than or equal to $(c^2E)^*_{cr}$, the motions of P_3 are limited outside of the orbits of P_2, which is similar to the case shown in Figure 9(a).

Besides, there is no exchange of the orbits of P_1 and P_2 based on the assumptions. Thus, the stability of the system is ensured.

Criterion II:

In the coplanar planetary four-body problem, three planets, P_1, P_2, P_3, orbit the star in a planetary hierarchy. P_1, P_2 are more massive than P_3 and the orbits of two massive planets are determined. The system is stable if

$$(c^2E)_{ac} \le (c^2E)^*_{cr}, \tag{45}$$

where $(c^2E)_{ac}$ is the actual value of c^2E of the system and $(c^2E)^*_{cr}$ is given by Equation (44).

Similarly, it is possible to express the real component of $\boldsymbol{\eta}_e$ and hence $(c^2E)^*_{cr}$ in a closed form. Denote $\boldsymbol{\eta}_e = x_e + iy_e$ and y_e is very small compared to x_e. Thus, we can set $\boldsymbol{\eta} = x$, where x is real and $x > 1$, and then the solution of the second of Equation (43), denoted as $\boldsymbol{\eta}_a$, is an approximation of $\boldsymbol{\eta}_e$.

The equilibrium point lies to the right side of P_2. Denote

$$x = 1 + \delta, \tag{46}$$

where $\delta > 0$ and usually $\delta < 0.1$. Substituting $\boldsymbol{\eta} = 1 + \delta$ and after some simplifications, the second of Equation (43) becomes

$$\begin{aligned}&\left[m_1\left|\boldsymbol{\xi}\right|^2 + m_2 + m_3(1+\delta)^2\right]\left[\frac{m_0m_3}{(1+\delta)^2} + \frac{m_2m_3}{\delta^2}\right] - \\ &m_3(1+\delta)\left[\frac{m_0m_1}{|\boldsymbol{\xi}|} + m_0m_2 + \frac{m_2m_3}{\delta} + \frac{m_0m_3}{1+\delta}\right] = 0.\end{aligned} \tag{47}$$

Then, by multiplying both sides of Equation (47) by $(1+\delta)^2\delta^2$, it becomes a univariate equation of five degrees, which is

$$\Sigma_{i=0}^5 d_i\delta^i = 0\,, \tag{48}$$

where

$$\begin{cases} d_5 = -\epsilon_2 - \epsilon_1/\left|\boldsymbol{\xi}\right|, \\ d_4 = -3\epsilon_2 - 3\epsilon_1/\left|\boldsymbol{\xi}\right|, \\ d_3 = -3\epsilon_2 - 3\epsilon_1/\left|\boldsymbol{\xi}\right|, \\ d_2 = (\left|\boldsymbol{\xi}\right|^2 - 1/\left|\boldsymbol{\xi}\right|)\epsilon_1, \\ d_1 = 3\epsilon_2\epsilon_3 + 2\epsilon_2^2 + 2\left|\boldsymbol{\xi}\right|^2\epsilon_1\epsilon_2, \\ d_0 = \epsilon_2\epsilon_3 + \epsilon_2^2 + \left|\boldsymbol{\xi}\right|^2\epsilon_1\epsilon_2, \end{cases} \tag{49}$$

and

$$\epsilon_1 = \frac{m_1}{m_0}, \quad \epsilon_2 = \frac{m_2}{m_0}, \quad \epsilon_3 = \frac{m_3}{m_0}. \tag{50}$$

In Equation (49) only the main items in the coefficients d_i are retained while the items with relatively smaller value are omitted. Furthermore, as m_0 is much larger than other bodies, the magnitude of the coefficients can be divided into different levels. The coefficients with a relatively large order of magnitude are d_5, d_4, d_3. The order of c_2 , c_1 and c_0 are associated with the parameter $|\boldsymbol{\xi}|$. Besides, the Hill sphere around P_2 is much smaller compared to the sphere around P_0 as the large mass of P_0, which means $\delta \ll 1$. We keep the smallest power in δ with the associated coefficient for the group of d_5, d_4, d_3. Therefore, the terms with the associated coefficient of d_5 and d_4 are neglected.

Thus, Equation (48) can be reduced to

$$d_3\delta^3 + d_2\delta^2 + d_1\delta + d_0 = 0. \tag{51}$$

Here the first and second order terms are retained as the coefficients d_1 and d_2 are related to the value of $|\boldsymbol{\xi}|$. It makes the relative error much bigger if these two terms are ignored.

Equation (51) is a cubic polynomial of δ and its roots can also be solved using Cardano's Formula. Therefore, an approximation to the solution of Equation (47) is given by

$$\begin{aligned}\delta_a = &\left(-\frac{t}{2} + \sqrt{\Delta_2}\right)^{1/3} + \left(-\frac{t}{2} - \sqrt{\Delta_2}\right)^{1/3} \\ &- \frac{d_2}{3d_3},\end{aligned} \tag{52}$$

where

$$\begin{cases} s = \dfrac{3d_3d_1 - d_2^2}{3d_3^2}\,, \\ t = \dfrac{27d_3^2d_0 - 9d_3d_2d_1 + 2d_2^3}{27d_3^3}\,, \end{cases} \tag{53}$$

and the discriminant of the cubic equation is

$$\Delta_2 = (s/3)^3 + (t/2)^2\,. \tag{54}$$

Then, the first line of Equation (43) can be expanded at the approximate solution $\boldsymbol{\eta}_a = 1 + \delta_a$, which is

$$\begin{aligned}\left(c^2E\right)^*_{cr,\boldsymbol{\xi}} = &\left(c^2E\right)^*_{\boldsymbol{\eta}_a} + \left[\left(c^2E\right)^*_{\boldsymbol{\eta}_a}\right]'(\boldsymbol{\eta}_e - \boldsymbol{\eta}_a) \\ &+ O\left((\boldsymbol{\eta}_e - \boldsymbol{\eta}_a)^2\right),\end{aligned} \tag{55}$$

where $\boldsymbol{\eta}_e$ denotes the exact solution of the second of Equation (43). Meanwhile, $\boldsymbol{\eta}_a = 1 + \delta_a$ is the approximation of the bifurcation point of the zero velocity surface, so $\left[\left(c^2E\right)^*_{\boldsymbol{\eta}_a}\right]' \approx 0$. Then Equation (55) becomes

$$\left(c^2E\right)^*_{cr,\boldsymbol{\xi}} = \left(c^2E\right)^*_{\boldsymbol{\eta}_a} + O\left((\boldsymbol{\eta}_e - \boldsymbol{\eta}_a)^2\right). \tag{56}$$

Thus, Equation (44) can be rewritten as

$$\begin{aligned}\left(c^2E\right)^*_{cr} = &-\frac{G^2m_0^5}{2} \\ &\times \max_{\boldsymbol{\xi}\in\Omega^*}\left\{\begin{aligned}&\left(\frac{\epsilon_1}{|\boldsymbol{\xi}|} + \epsilon_2 + \frac{\epsilon_2\epsilon_3}{\delta_a} + \frac{\epsilon_3}{1+\delta_a}\right)^2 \times \\ &\times\left[\epsilon_1\left|\boldsymbol{\xi}\right|^2 + \epsilon_2 + \epsilon_3(1+\delta_a)^2\right]\end{aligned}\right\},\end{aligned} \tag{57}$$

where Ω^* is the range of $\boldsymbol{\xi}$.

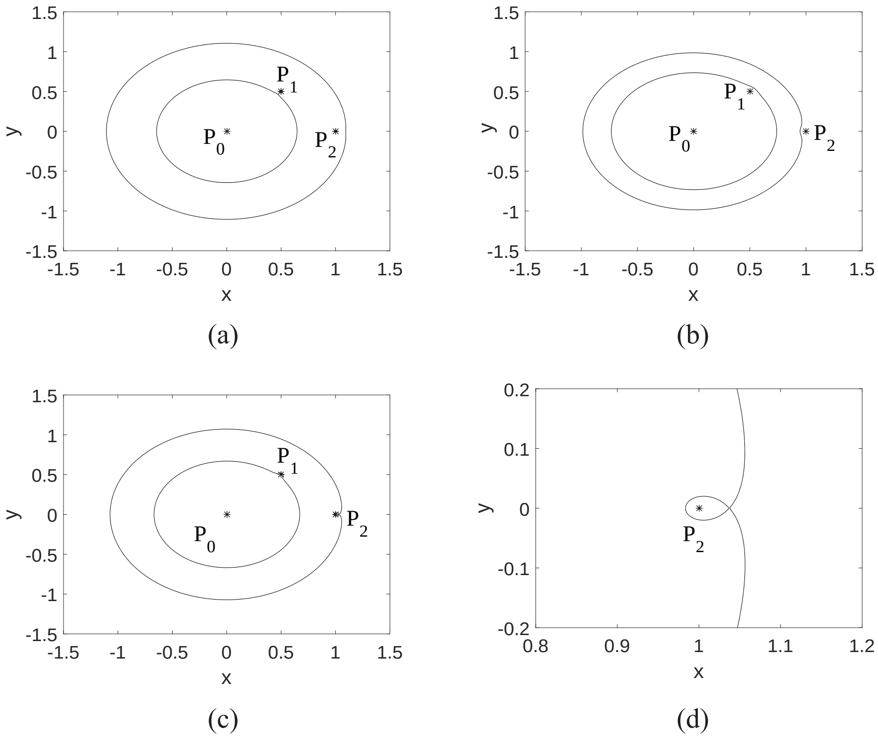

Fig. 9 Zero velocity curves of P_3. (a) $c^2E = -4.44 \times 10^{-9}$, (b) $c^2E = -4.41 \times 10^{-9}$, (c) $c^2E = -4.4299380 \times 10^{-9}$, (d) $c^2E = -4.4299380 \times 10^{-9}$, around P_3. $G = 1$, $m_0 = 1$, $m_1 = m_2 = 9.55206 \times 10^{-4}$, $m_3 = 9.55206 \times 10^{-5}$, $\boldsymbol{\xi} = 0.5 + 0.5i$. The values of parameter c^2E are given in each subfigure.

The value of $(c^2E)^*_{cr}$ monotonically increases with $|\boldsymbol{\xi}|$ when

$$|\boldsymbol{\eta}| \leq \left(\frac{\epsilon_2 + \epsilon_3(1+\delta_a)^2}{\epsilon_2 + \epsilon_3/(1+\delta_a) + \epsilon_2\epsilon_3/\delta_a} \right)^{1/3} . \tag{58}$$

The right side of inequality (58) is greater than 1 as three mass parameters are much smaller than δ_a. As P_1 locates inside of the orbit of P_2, $|\boldsymbol{\xi}| < 1$. Therefore, denote $\rho_m = \min |\boldsymbol{\xi}|$, and Equation (57) becomes

$$\begin{aligned} (c^2E)^*_{cr} = & -\frac{G^2 m_0^5}{2} \\ & \left\{ \left(\frac{\epsilon_1}{\rho_m} + \epsilon_2 + \frac{\epsilon_2\epsilon_3}{\delta_a} + \frac{\epsilon_3}{1+\delta_a} \right)^2 \times \right. \\ & \left. \times \left[\epsilon_1\rho_m^2 + \epsilon_2 + \epsilon_3(1+\delta_a)^2 \right] \right\} . \end{aligned} \tag{59}$$

The value determined by Equation (59) also is an approximation of the exact critical value. The accuracy has been verified with the results shown in Figure 10. The relative error compared to the exact value tends to be less than 0.005 which means the approximation is also reasonable.

In Criterion II, the actual value $(c^2E)_{ac}$ can also be expressed by Equation (37). Substitutions of Equations (37) and (59) into the stability condition (45) give

$$D(1-e_3^2) + E\sqrt{1-e_3^2} + F \geq 0 , \tag{60}$$

where

$$\left\{ \begin{aligned} D = & (\epsilon_1/\alpha_{12} + \epsilon_2 + \epsilon_3/\alpha_{32})\, \epsilon_3^2 \alpha_{32} , \\ E = & 2 \left[\epsilon_1 \sqrt{\alpha_{12}(1-e_1^2)} + \epsilon_2\sqrt{1-e_2^2} \right] \\ & \times (\epsilon_1/\alpha_{12} + \epsilon_2 + \epsilon_3/\alpha_{32})\, \epsilon_3 \sqrt{\alpha_{32}} , \\ F = & \left[\epsilon_1 \sqrt{\alpha_{12}(1-e_1^2)} + \epsilon_2\sqrt{1-e_2^2} \right]^2 \\ & \times (\epsilon_1/\alpha_{12} + \epsilon_2 + \epsilon_3/\alpha_{32}) \\ & - \left(\frac{\epsilon_1}{\rho_m} + \epsilon_2 + \frac{\epsilon_2\epsilon_3}{\delta_a} + \frac{\epsilon_3}{1+\delta_a} \right)^2 \\ & \times \left[\epsilon_1\rho_m^2 + \epsilon_2 + \epsilon_3(1+\delta_a)^2 \right] . \end{aligned} \right. \tag{61}$$

If $F \geq 0$ inequality (60) holds as $D > 0$ and $E > 0$. If $F < 0$, this gives a solution of the form

$$e_3 \leq \sqrt{1 - \left(\frac{-E + \sqrt{E^2 - 4DF}}{2D} \right)^2} . \tag{62}$$

The $\alpha_{32} - e_3$ curves for different values of α_{12} are shown in Figure 11. The regions below the curves are stable. The outer planet with a small eccentricity is more likely to be stable. The stable regions increase if the parameter α_{12} increases. The relations between α_{12} and α_{32} are shown in Figure 12. The region on the upper side of the

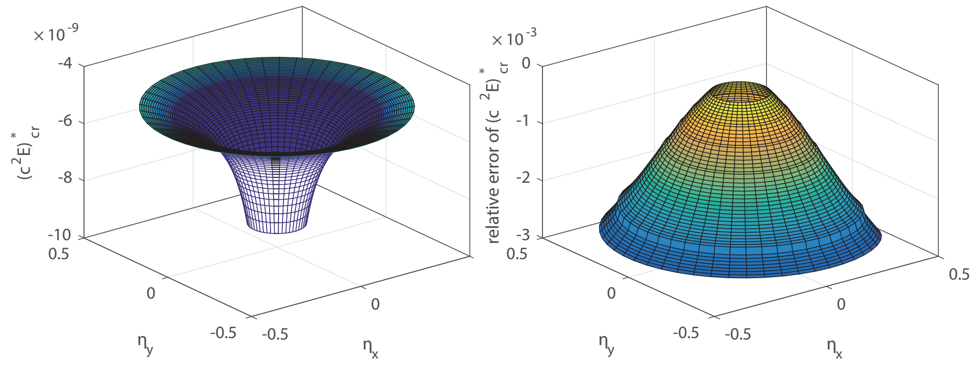

Fig. 10 Comparison of the approximation and the exact solution of $(c^2E)^*_{cr}$. (a) Approximation and exact solution of $(c^2E)^*_{cr}$, (b) relative error of $(c^2E)^*_{cr}$. $G = 1$, $m_0 = 1$, $m_1 = 10^{-3}$, $m_2 = 10^{-3}$, $m_3 = 10^{-4}$, and $0.1 < |\boldsymbol{\xi}| < 0.5$. In Fig. 10(a) the two surfaces are too close to distinguish. Fig. 10(b) shows the relative error between the approximation and the exact value of $(c^2E)^*_{cr}$.

curve is ensured to be stable with the conditions $\alpha_{32} > 1$ and $\alpha_{12} < 1$. The plot makes it clear that with the increases of the parameter α_{12} the value of α_{32} decreases which means the ensured stable regions have increased.

This is the same as saying that the stability criterion is sufficient but not necessary. We can conclude that the stable regions in Figure 11 absolutely are stable. Nevertheless, the real stable regions may be larger than that the criterion gives. Therefore, the trend shown in Figure 12 represents the results of the criterion but it may be not real situations.

If $m_1 = 0$, the problem degenerates into a three-body case. Similarly, the stable regions in the $\alpha_{32} - e_3$ plane are shown in Figure 13. The solid line is the boundary of the three-body problem while the others are the boundaries for different α_{12} in the four-body case. In general, the inner planet reduces the stable regions of the outer planet which makes the stability worse.

4 APPLICATION TO THE SOLAR SYSTEM AND EXTRASOLAR PLANETARY SYSTEMS

The stability criteria are applied to the Solar System, as the orbits of the planets in the Solar System are approximately coplanar, and there is no cross of planets' orbits. Therefore, the Solar System can be divided into different planetary four-body systems.

As Jupiter and Saturn are more massive than the other planets, it is reasonable that all the combinations of the four-body system include Jupiter and Saturn. For a Sun-Planet-Jupiter-Saturn (or Sun-Jupiter-Saturn-Planet) system, using the criterion obtained in Section 3.1 (or Sect. 3.2), the results are shown in Table 1.

Table 1 Stability of the Planetary Four-body Systems in the Solar System

P_1	P_2	P_3	Criterion I or II
Mercury	Jupiter	Saturn	Unsatisfied
Venus	Jupiter	Saturn	Unsatisfied
Earth	Jupiter	Saturn	Unsatisfied
Mars	Jupiter	Saturn	Unsatisfied
Jupiter	Saturn	Uranus	Unsatisfied
Jupiter	Saturn	Neptune	Unsatisfied

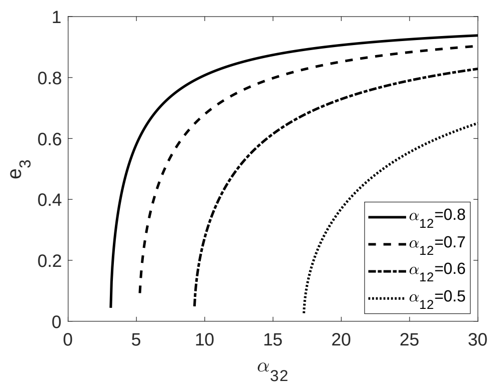

Fig. 11 The $\alpha_{32} - e_3$ curves for different value of α_{12}. The parameters of the system are given as $G = 1$, $m_0 = 1$, $m_1 = 10^{-3}$, $m_2 = 10^{-3}$, $m_3 = 10^{-4}$, $e_1 = 0.02$, and $e_2 = 0.02$. Here $\alpha_{12} = a_1/a_2$ and $\alpha_{32} = a_3/a_2$. The regions below the curves are ensured to be stable.

All of the systems listed in Table 1 do not satisfy Criterion I or II. The system still could be stable as the criterion is a sufficient condition but not necessary.

Now we will consider the possible applications of the stability to extrasolar systems. There are 672 multiple-planet systems listed at the website *http://exoplanet.eu/catalog/*. Among them, five four-

Table 2 Stability of the Five Extrasolar Four-body Systems

Star (1)	Planet (2)	M_p ($M_{\rm Jup}$) (3)	a_p (AU) (4)	e_p (5)	$M_{\rm star}$ ($M_{\rm Sun}$) (6)	$(c^2E)_{ac}$ (7)	$(c^2E)_{cr}$ or $(c^2E)^*_{cr}$ (8)	Criterion I or II (9)	Integration Results (10)
	GJ 676 A d	0.014	0.0413	0.1500					
GJ 676 A	GJ 676 A b	6.7	1.8120	0.3230	0.7251	–9.1502e-06	–2.00563e-05	unsatisfied	unstable
	GJ 676 A c	6.8	6.6000	0.2000					
	GJ 876 d	0.022	0.0208	0.0810					
GJ 876	GJ 876 c	0.856	0.1296	0.0020	0.3193	–4.61805e-07	–3.45491e-07	satisfied	stable
	GJ 876 b	1.94	0.2083	0.0000					
	HD 125612 c	0.058	0.0500	0.2700					
HD 125612	HD 125612 b	3	1.3700	0.4600	0.9660	–1.70786e-06	–3.04841e-06	unsatisfied	unstable
	HD 125612 d	7.2	4.2000	0.2800					
	PSR 1257 12 b	7e-05	0.1900	0.0000					
PSR 1257 12	PSR 1257 12 c	0.013	0.3600	0.0186	1.4337	–2.67709e-15	–2.476e-15	satisfied	stable
	PSR 1257 12 d	0.012	0.4600	0.0252					
	ups And b	0.62	0.0590	0.0119					
ups And	ups And c	9.1	0.8610	0.2445	1.2851	–2.66322e-05	–2.72339e-05	unsatisfied	unstable
	ups And d	23.6	2.5500	0.3160					

The four-body systems consist of a star and three planets, which are shown in Cols (1)–(2). The mass of the planet in Col (3) is shown in the unit of Jupiter mass, while in Col. (6) the mass of the star is in the unit of Sun mass. a_p and e_p in Cols. (4)–(5) are semi-major axis and eccentricity of the planet, respectively. The mass and the orbital parameters of the systems are obtained by the website *http://exoplanet.eu/catalog/*. The last column lists the numerical integration results by using the N-body integrator.

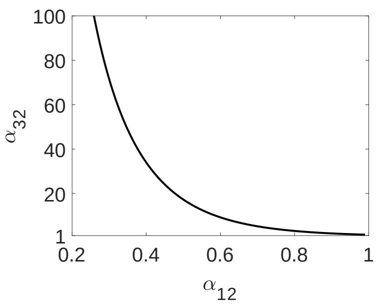

Fig. 12 The $\alpha_{12} - \alpha_{32}$ curve. The parameters of the system are given as $G = 1$, $m_0 = 1$, $m_1 = 10^{-3}$, $m_2 = 10^{-3}$, $m_3 = 10^{-4}$, and $e_1 = e_2 = e_3 = 0.02$. Here $\alpha_{12} = a_1/a_2$ and $\alpha_{32} = a_3/a_2$. The regions on the upper side of the curve are ensured to be stable with the conditions $\alpha_{32} > 1$ and $\alpha_{12} < 1$.

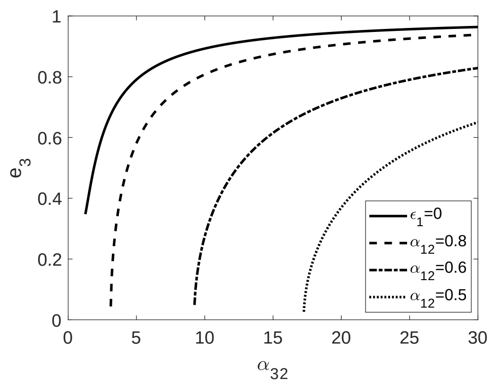

Fig. 13 The $\alpha_{32} - e_3$ curves. The parameters of the four-body system are given as $G = 1$, $m_0 = 1$, $m_1 = 10^{-3}$, $m_2 = 10^{-3}$, $m_3 = 10^{-4}$, and $e_1 = e_2 = 0.02$. Here $\alpha_{12} = a_1/a_2$ and $\alpha_{32} = a_3/a_2$. For the three-body case, $m_1 = 0$. The regions on the right side of the curves are ensured to be stable.

body systems satisfy the conditions that three planets orbit the star without orbits crossing and two of the planets in the systems are 10 times massive than the third one.

Criterion I and II are applied to these systems and the results are shown in Table 2. Criterion I (or II) determines the value of $(c^2E)_{cr}$ (or $(c^2E)^*_{cr}$). The expression of the actual value $(c^2E)_{ac}$ is given by Equation (37).

Two of the planetary systems, GJ 876^{d,c,b}, PSR 1257 12^{b,c,d}, listed in Table 2 satisfy the Criterion I or II, which means they are stable. The motions of the smallest planet are bounded by the orbit of its massive planetary neighbor. The other systems where the criteria are unsatisfied have the possibility to change their order of planetary orbits.

The results are checked by the direct N-body integrations. The systems are integrated with the Mercury integrator package (Chambers & Migliorini 1997) using the Bulirsch-Stoer integrator (Stoer & Bulirsch 1980). We adopt a timestep as 0.02 times of the period of the inner planet. The integrations continue until the orbits of two or more planets cross or 10^6 inner orbital periods elapse. A closer encounter is defined as the distance between any pair of planets become less than the sum of the Hill radius of the two planets, while the Hill radius is given by $R_H = a\,(\mu/3)^{1/3}$, where a is the semi-major axis and μ is the dimensionless mass. As shown in the last column of Table 2, the integration results match the criteria well. For the systems which satisfy the criteria, they are ensured to be stable if the orbits of the massive planets keep unchanged. For those unsatisfied with the criteria, they become unstable obviously during the integrations.

5 CONCLUSIONS

This work concentrates on the stability of the coplanar planetary four-body problem by studying the topology of the regions of possible motions.

For a planetary four-body system, two stability criteria are obtained. The special systems which satisfy Criteria I and II are definitely to be stable under the definition. Criteria I and II are appropriate for the case that two of the planets with known orbits are more massive than the third one. There is a critical constant, and if the actual value of c^2E is less than or equal to the critical constant, the motions of the third planet are bounded and hence the system is stable.

All of the combinations in the Solar System listed in Table 1 are unsatisfied. Two of the extrasolar systems listed in Table 2 are stable. The applications of the criteria are limited as the simplification by fixing the two massive planets on determined orbits. In fact, the criteria are applicative even if we just know the regions of motions of the massive planets. Besides, as the planetary three-body problem has been well studied, the motions of the sub-system consisting of the star and the two massive planets could be studied first, which makes the applications more reasonable.

Acknowledgements This work was supported by the National Natural Science Foundation of China (Grant Nos. 11772167 and 11822205). The authors would like to thank the anonymous referees for their very careful reviews that include many important points and will improve significantly the clarity of this paper.

References

Bozis, G. 1976, Astrophysics Space Science, 43, 355
Chambers, J., & Migliorini, F. 1997, Bull. Am. Astron. Soc., 29, 1024
Chambers, J., Wetherill, G., & Boss A. 1996, Icarus, 119, 261
Donnison, J. R. 1984a, Celestial Mechanics, 32, 145
Donnison, J. R. 1984b, MNRAS, 210, 915
Donnison, J. R. 1988, MNRAS, 231, 85
Donnison, J. R. 2006, MNRAS, 369, 1267
Donnison, J. R. 2009, Planetary and Space Science, 57, 771
Donnison, J. R. 2010, MNRAS, 406, 1918
Donnison, J. R. 2011, MNRAS, 415, 470
Donnison, J. R., & Mikulskis, D. F. 1992, MNRAS, 254, 21
Donnison, J. R., & Mikulskis D. F. 1994, MNRAS, 266, 25
Donnison, J. R., & Williams, I. P. 1983, Celestial Mechanics, 31, 123
Donnison, J. R., & Williams, I. P. 1985, MNRAS, 215, 567
Duncan, M. J., & Lissauer, J. J. 1997, Icarus, 125, 1
Faber, P., & Quillen, A. C. 2007, MNRAS, 382, 1823
Golubev, V. G. 1967, Soviet Physics Doklady, 12, 529
Golubev, V. G. 1968a, Soviet Physics Doklady, 13, 373
Golubev, V. G. 1968b, Doklady. Akad. Nauk., 180, 308
Gong, S., & Liu, C. 2016, MNRAS, 462, 547
Harrington, R. S. 1972, Celestial Mechanics, 6, 322
Hill, G. W. 1878, American Journal of Mathematics, 1, 5
Liu, C., & Gong, S. 2017a, Astrophysics and Space Science, 362, 127
Liu, C., & Gong, S. 2017b, MNRAS, 469, 3576
Lukyanov, L. G., & Uralskaya, V. S. 2012, MNRAS, 421, 2316
Marchal, C., & Bozis, G. 1982, Celestial Mechanics, 26, 311
Marchal, C., & Saari, D. G. 1975, Celestial Mechanics, 12, 115
Obertas, A., Van Laerhoven, C., & Tamayo D. 2017, Icarus, 293, 52
Petit, A. C., Laskar, J., Boué, G. 2018, A&A, 617, A93
Saari, D. G. 1974, SIAM J. Appl. Math., 26, 806
Saari, D. G. 1984, Celestial Mechanics, 33, 299
Saari, D. G. 1987, Celestial Mechanics, 40, 197
Sergysels, R. 1986, Celestial Mechanics, 38, 207
Smith A. W., Lissauer J. J. 2009, Icarus, 201, 381
Sosnitskii S. P. 1999, Astronomical Journal, 117, 3054
Stoer, J., & Bulirsch, R. 1980, Introduction to Numerical Analysis (New York: Springer-Verlag)
Sundman, K. F. 1912, Acta Mathematica, 36, 105
Szebehely, V. 1977, Celestial Mechanics, 15, 107
Szebehely, V., & Zare, K. 1977, Astronomy Astrophysics, 58, 145
Tamayo, D., et al. 2016, The Astrophysical Journal Letters, 832, L22
Walker, I. W. 1983a, Celestial Mechanics, 29, 149
Walker, I. W. 1983b, Celestial Mechanics, 29, 215
Walker, I. W., & Roy, A. E. 1981, Celestial Mechanics, 24, 195
Walker, I. W., & Roy, A. E. 1983a, Celestial Mechanics, 29, 117
Walker, I. W., & Roy, A. E. 1983b, Celestial Mechanics, 29, 267
Walker, I. W., Emslie, A. G., & Roy, A. E. 1980, Celestial Mechanics, 22, 371
Zare, K. 1976, Celestial Mechanics, 14, 73
Zare, K. 1977, Celestial Mechanics, 16, 35